Development of Steel Representation as Embedded Bars in Concrete Using Finite Element Method

Dr. Zubaidah A. Al-Bayati
Civil Engineering Dept., College of Engineering
Al-Mustansiriya University, Baghdad, Iraq

Eng. Jassim Jarallah Fahed
Civil Engineering Dept., College of Engineering
Al-Mustansiriya University, Baghdad, Iraq

Abstract

A new model for embedded bar formulation in the finite element analysis is presented, this new model differs from the conventional models, that it can represent the bar in more accurate way, also it can deal with curved and/or complicated bar geometry.

The current formulation is made using finite element analysis by considering the degenerated assumed strain eight-noded shell finite element with each node having five degrees of freedom and nonlinear material properties and solution techniques.

The validity of the current formulation is proved through comparing the results obtained from the generated computer program with that of experimentally tested slabs by different researches.

الخلاصـــــة

في البحث الحالي تم تقديم طريقة جديدة لتمثيل القضيب المطمور باستخدام طريقة العناصر المحددة. الطريقة الحالية تختلف عن الطرق التقليدية الاخرى بكونها تستطيع تمثيل القضيب بدقة اكثر كما و تستطيع التعامل مع شكل القضيب المنحني او اي شكل اخر.

تم استخدام العنصر القشري المولد و المؤلف من ثمانية عقد و لكل عقدة خمسة درجات حرية للحركة مع تمثيل المادة بخواصها اللاخطية و استخدام طرق حل لا خطية ايضاً.

تم اثبات صحة الطريقة المقترحة بمقارنة النتائج المستحصلة من البرنامج المعد مع النتائج العملية لعدد من السقوف الانشائية المفحوصة مختبرياً من قبل باحثين اخرين.

1. Introduction

In the nonlinear finite element analysis of reinforced thin plate structures, the steel reinforcement is usually represented as a smeared layer. Alternatively, when there is a lumped area of steel at a certain location, like the main steel bars in beams or prestressing tendons, the reinforcement is usually represented as a single discrete bar element connected to the nodes of the adjacent concrete elements. The discrete modeling of the steel reinforcement is the first approach used in the finite element analysis of reinforced concrete structures, which was originally suggested by Ngo and Scordelis [1].

When shell elements are used to model reinforced concrete structures, the discrete bar representation of steel suffers from the following drawbacks:

1. In the case of curved or complicated bar geometry a distorted shell element needs to be used to match the bar geometry.
2. The bar must be assumed to lie in the mid-surface of the shell element, as shown in **Fig.(1)**, where the nodes of the parent element are located. So the finite element mesh patterns are restricted by the location of reinforcement and consequently the increase in the number of concrete elements and degrees of freedom [2].

In order to achieve the advantages of a regular mesh, and at the same time model complicated reinforcing details, an embedded representation of reinforcement appears to be the desirable approach. Even so, the present embedded reinforcement models, when applied to problems with curved or draped reinforcement and prestressing tendons impose significant constraints on the selection of the overall mesh. A need therefore exists, for curved embedded representation of reinforcement that allows the choice of mesh to be somewhat independent of the reinforcement geometry and location.

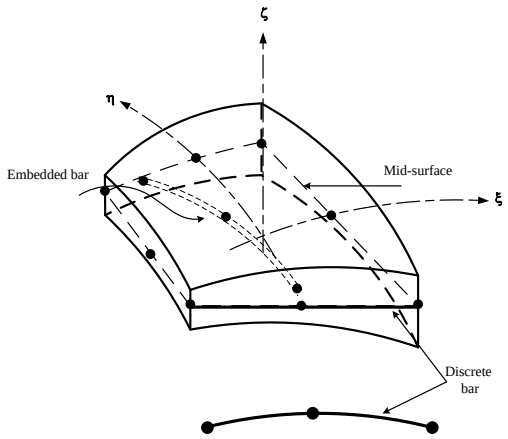

Figure (1) Embedded and discrete bar element in shell element

Over the past decades, a number of embedded representations for reinforcement have been published [3, 4, 5, 6].

Phillips and Zienkiewicz [3], introduced the embedded representation of reinforcement. In their derivation, the reinforcing bar is restricted to lie along the local coordinates, ξ or η

of the parent element. Ranjbaran [6], modified the representation adopted above to account for inclined bars, using one-dimensional bar element with two nodes embedded in 8-noded two-dimensional concrete element. The current formulation is based on modifying the above representation by using three-noded one-dimensional bar element embedded in the degenerated concrete shell element shown in **Fig.(2)**, which can represent inclined and/or curved tendons, using two Gaussian points.

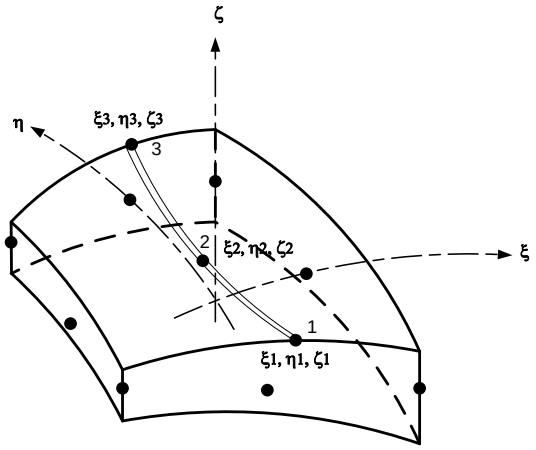

Figure (2) Three-noded bar element embedded in the degenerated shell element

2. Assumptions

The following assumptions are made:

1. Full bond occurs between the tendons and the concrete, i.e. slip of tendons relative to concrete is ignored.
2. Compatibility of tendons and concrete deformations necessitates that the strain of concrete and tendons at common points to be the same.

3. Basic Formulation

In the degenerated shell elements, it is assumed that, the strain energy corresponding to stresses perpendicular to the middle surface is disregarded, i.e. the stress component normal to the shell mid-surface is constrained to be zero in the constitutive equations. In order to more easily deal with the shell assumption of zero normal stress in the $\mathbf{z'}$-direction $\boldsymbol{\sigma_{z'} = 0}$, the strain components should be defined in terms of the local system of axes $\mathbf{x'_1}$ (where $\mathbf{x'_3 = z'}$ is perpendicular to the $\xi\eta$-plane).The local system of axes is also the most convenient system for expressing the stress components (and their resultants) for shell analysis and design. The five significant strain components are:

$$\varepsilon = \begin{Bmatrix} \varepsilon_{x'} \\ \varepsilon_{y'} \\ \gamma_{x'y'} \\ \gamma_{x'z'} \\ \gamma_{y'z'} \end{Bmatrix} = \begin{Bmatrix} \dfrac{\partial u'}{\partial x'} \\ \dfrac{\partial v'}{\partial y'} \\ \dfrac{\partial u'}{\partial y'} + \dfrac{\partial v'}{\partial x'} \\ \dfrac{\partial u'}{\partial z'} + \dfrac{\partial w'}{\partial x'} \\ \dfrac{\partial v'}{\partial z'} + \dfrac{\partial w'}{\partial y'} \end{Bmatrix} \quad \text{..... (1)}$$

where, $\mathbf{u', v'}$ and $\mathbf{w'}$ are the displacement components in the local system $\mathbf{x'_i}$. These local derivatives are obtained from the global derivatives of the displacements **u**, **v**, and **w** by the following operation:

$$\begin{bmatrix} \dfrac{\partial u'}{\partial x'} & \dfrac{\partial v'}{\partial x'} & \dfrac{\partial w'}{\partial x'} \\ \dfrac{\partial u'}{\partial y'} & \dfrac{\partial v'}{\partial y'} & \dfrac{\partial w'}{\partial y'} \\ \dfrac{\partial u'}{\partial z'} & \dfrac{\partial v'}{\partial z'} & \dfrac{\partial w'}{\partial z'} \end{bmatrix} = [\theta]^T \begin{bmatrix} \dfrac{\partial u}{\partial x} & \dfrac{\partial v}{\partial x} & \dfrac{\partial w}{\partial x} \\ \dfrac{\partial u}{\partial y} & \dfrac{\partial v}{\partial y} & \dfrac{\partial w}{\partial y} \\ \dfrac{\partial u}{\partial z} & \dfrac{\partial v}{\partial z} & \dfrac{\partial w}{\partial z} \end{bmatrix} [\theta] \quad \text{..... (2)}$$

where, $[\theta]$ is a transformation matrix defined as:

$$[\theta] = [\bar{x}', \bar{y}', \bar{z}'] \quad \text{..... (3.a)}$$

where, $\bar{x}', \bar{y}'$ and $\bar{z}'$ are unit vectors in the direction of $\mathbf{x'}, \mathbf{y'}$ and $\mathbf{z'}$ axes, respectively.

$$\theta = \begin{bmatrix} \dfrac{\partial x}{\partial x'} & \dfrac{\partial x}{\partial y'} & \dfrac{\partial x}{\partial z'} \\ \dfrac{\partial y}{\partial x'} & \dfrac{\partial y}{\partial y'} & \dfrac{\partial y}{\partial z'} \\ \dfrac{\partial z}{\partial x'} & \dfrac{\partial z}{\partial y'} & \dfrac{\partial z}{\partial z'} \end{bmatrix} \quad \text{..... (3.b)}$$

Since only the longitudinal strain ε'_x in the embedded bar is considered, this is the first term in the matrix of Equation (2):

$$\varepsilon'_x = {}^{\partial u'}\!/_{\partial x'} \quad \text{..... (4)}$$

Expansion of the above Equation yields:

$$\left.\begin{aligned}\frac{\partial u'}{\partial x'} &= \left(\frac{\partial u}{\partial x}\right)\left(\frac{\partial u}{\partial x'}\right)\left(\frac{\partial x}{\partial x'}\right)+\left(\frac{\partial u}{\partial y}\right)\left(\frac{\partial y}{\partial x'}\right)\left(\frac{\partial x}{\partial x'}\right)+\left(\frac{\partial u}{\partial z}\right)\left(\frac{\partial z}{\partial x'}\right)\left(\frac{\partial x}{\partial x'}\right)\\ &+\left(\frac{\partial v}{\partial x}\right)\left(\frac{\partial x}{\partial x'}\right)\left(\frac{\partial y}{\partial x'}\right)+\left(\frac{\partial v}{\partial y}\right)\left(\frac{\partial y}{\partial x'}\right)\left(\frac{\partial y}{\partial x'}\right)+\left(\frac{\partial v}{\partial z}\right)\left(\frac{\partial z}{\partial x'}\right)\left(\frac{\partial y}{\partial x'}\right)\\ &+\left(\frac{\partial w}{\partial x}\right)\left(\frac{\partial x}{\partial x'}\right)\left(\frac{\partial z}{\partial x'}\right)+\left(\frac{\partial w}{\partial y}\right)\left(\frac{\partial y}{\partial x'}\right)\left(\frac{\partial z}{\partial x'}\right)+\left(\frac{\partial w}{\partial z}\right)\left(\frac{\partial z}{\partial x'}\right)\left(\frac{\partial z}{\partial x'}\right)\end{aligned}\right\} \quad \text{..... (5)}$$

Rewriting the direction cosine matrix in the following form:

$$\theta^T = \begin{bmatrix} \ell_1 & m_1 & n_1 \\ \ell_2 & m_2 & n_2 \\ \ell_3 & m_3 & n3 \end{bmatrix} \quad \text{..... (6)}$$

where:

$$\left.\begin{aligned}\ell_1 &= \frac{\partial x}{\partial x'}\\ m_1 &= \frac{\partial y}{\partial x'}\\ n_1 &= \frac{\partial z}{\partial x'}\end{aligned}\right\} \quad \text{..... (7)}$$

thus,

$$\left.\begin{aligned}\frac{\partial u'}{\partial x'} &= \left(\frac{\partial u}{\partial x}\right)\ell_1^2+\left(\frac{\partial u}{\partial y}\right)\ell_1 m_1+\left(\frac{\partial u}{\partial z}\right)\ell_1 n_1+\left(\frac{\partial v}{\partial x}\right)\ell_1 m_1+\left(\frac{\partial v}{\partial y}\right)m_1^2\\ &+\left(\frac{\partial v}{\partial z}\right)m_1 n_1+\left(\frac{\partial w}{\partial x}\right)\ell_1 n_1+\left(\frac{\partial w}{\partial y}\right)m_1 n_1+\left(\frac{\partial w}{\partial z}\right)n_1^2\end{aligned}\right\} \quad \text{..... (8)}$$

i.e.

$$\left.\begin{aligned}\varepsilon_x' &= \varepsilon_x\ell_1^2+\varepsilon_y m_1^2+\varepsilon_z n_1^2+\left(\frac{\partial u}{\partial y}+\frac{\partial v}{\partial x}\right)\ell_1 m_1\\ &+\left(\frac{\partial u}{\partial z}+\frac{\partial w}{\partial x}\right)\ell_1 n_1+\left(\frac{\partial v}{\partial z}+\frac{\partial w}{\partial y}\right)m_1 n_1\end{aligned}\right\} \quad \text{..... (9)}$$

The definition of **u**, **v**, and **w** at node k in the degenerated shell element are given by the following Equation:

$$\begin{Bmatrix} u \\ v \\ w \end{Bmatrix} = \begin{bmatrix} N_k & 0 & 0 & N_k\zeta\frac{h_k}{2}v_{1k}^x & -N_k\zeta\frac{h_k}{2}v_{2k}^x \\ 0 & N_k & 0 & N_k\zeta\frac{h_k}{2}v_{1k}^y & -N_k\zeta\frac{h_k}{2}v_{2k}^y \\ 0 & 0 & N_k & N_k\zeta\frac{h_k}{2}v_{1k}^z & -N_k\zeta\frac{h_k}{2}v_{2k}^y \end{bmatrix} \begin{Bmatrix} u_k \\ v_k \\ w_k \\ \beta_k \\ \alpha_k \end{Bmatrix} \quad \text{..... (10)}$$

Substituting these values of **u**, **v**, and **w** into Equation (9) yields:

$$\varepsilon'_x = \begin{bmatrix} B_{P11} & B_{P12} & B_{P13} & B_{P14} & B_{P15} \end{bmatrix} \begin{Bmatrix} u_i \\ v_i \\ w_i \\ \beta_i \\ \alpha_i \end{Bmatrix} \quad \text{..... (11)}$$

where:

$$B_{P11} = \frac{\partial N_i}{\partial x}\ell_1^2 + \frac{\partial N_i}{\partial y}\ell_1 m_1 + \frac{\partial N_i}{\partial z}\ell_1 n_1 \quad \text{..... (12)}$$

$$B_{P12} = \frac{\partial N_i}{\partial x}\ell_1 m_1 + \frac{\partial N_i}{\partial y}m_1^2 + \frac{\partial N_i}{\partial z}m_1 n_1 \quad \text{..... (13)}$$

$$B_{P13} = \frac{\partial N_i}{\partial x}\ell_1 n_1 + \frac{\partial N_i}{\partial y}m_1 n_1 + \frac{\partial N_i}{\partial z}n_1^2 \quad \text{..... (14)}$$

$$\left.\begin{aligned} B_{P14} = {} & \tfrac{\partial N_i}{\partial x}\zeta\tfrac{h}{2}\left[v_{1i}^x\ell_1^2 + v_{1i}^y\ell_1 m_1 + v_{1i}^z\ell_1 n_1\right] + \tfrac{\partial N_i}{\partial y}\zeta\tfrac{h}{2} \\ & \left[v_{1i}^x\ell_1 m_1 + v_{1i}^y m_1^2 + v_{1i}^z m_1 n_1\right] + \tfrac{\partial N_i}{\partial z}\zeta\tfrac{h}{2}\left[v_{1i}^x\ell_1 n_1 + v_{1i}^y m_1 n_1 + v_{1i}^z n_1^2\right] \end{aligned}\right\} \quad \text{..... (15)}$$

$$\left.\begin{aligned} B_{P15} = {} & -\tfrac{\partial N_i}{\partial x}\zeta\tfrac{h}{2}\left[v_{2i}^x\ell_1^2 + v_{2i}^y\ell_1 m_1 + v_{2i}^z\ell_1 n_1\right] - \tfrac{\partial N_i}{\partial y}\zeta\tfrac{h}{2} \\ & \left[v_{2i}^x\ell_1 m_1 + v_{2i}^y m_1^2 + v_{2i}^z m_1 n_1\right] - \tfrac{\partial N_i}{\partial z}\zeta\tfrac{h}{2}\left[v_{2i}^x\ell_1 n_1 + v_{2i}^y m_1 n_1 + v_{2i}^z n_1^2\right] \end{aligned}\right\} \quad \text{..... (16)}$$

A dimensionless coordinate τ is defined along the embedded bar in the parent element ($-1 < \tau < 1$). Since x' coincides with τ except for a coefficient, then:

$$\ell_1 = \frac{\partial x}{\partial x'} = \frac{\partial x}{\partial \tau}\frac{\partial \tau}{\partial x'} = \frac{1}{c}\frac{\partial x}{\partial \tau} \quad \text{..... (17)}$$

$$m_1 = \frac{\partial y}{\partial x'} = \frac{\partial y}{\partial \tau}\frac{\partial \tau}{\partial x'} = \frac{1}{c}\frac{\partial y}{\partial \tau} \quad \text{..... (18)}$$

$$n_1 = \frac{\partial z}{\partial x'} = \frac{\partial z}{\partial \tau}\frac{\partial \tau}{\partial x'} = \frac{1}{c}\frac{\partial z}{\partial \tau} \quad \text{..... (19)}$$

Since,

$$\ell_1^2 + m_1^2 + n_1^2 = 1 \quad \text{..... (20)}$$

$$\therefore \quad c = \sqrt{\left(\frac{\partial x}{\partial \tau}\right)^2 + \left(\frac{\partial y}{\partial \tau}\right)^2 + \left(\frac{\partial z}{\partial \tau}\right)^2} \quad \text{..... (21)}$$

So the Jacobian may be evaluated as:

$$\left|J_P\right| = \left|\frac{dx}{d\tau}\right| = c \quad \text{..... (22)}$$

Letting:

$$c_1 = \left(\frac{\partial x}{\partial \tau}\right)^2 \quad \text{..... (23)}$$

$$c_2 = \left(\frac{\partial x}{\partial \tau}\right)\left(\frac{\partial y}{\partial \tau}\right) \quad \text{..... (24)}$$

$$c_3 = \left(\frac{\partial x}{\partial \tau}\right)\left(\frac{\partial z}{\partial \tau}\right) \quad \text{..... (25)}$$

$$c_4 = \left(\frac{\partial y}{\partial \tau}\right)^2 \quad \text{..... (26)}$$

$$c_5 = \left(\frac{\partial y}{\partial \tau}\right)\left(\frac{\partial z}{\partial \tau}\right) \quad \text{..... (27)}$$

$$c_6 = \left(\frac{\partial z}{\partial \tau}\right)^2 \quad \text{..... (28)}$$

Thus:

$$\ell_1^2 = \frac{1}{c^2} c_1 \quad \text{..... (29)}$$

$$m_1^2 = \frac{1}{c^2} c_4 \quad \text{..... (30)}$$

$$n_1^2 = \frac{1}{c^2} c_6 \quad \text{..... (31)}$$

$$\ell_1 m_1 = \frac{1}{c^2} c_2 \quad \text{..... (32)}$$

$$\ell_1 n_1 = \frac{1}{c^2} c_3 \quad \text{..... (33)}$$

$$m_1 n_1 = \frac{1}{c^2} c_5 \quad \text{..... (34)}$$

Let $\tilde{a} = \zeta \frac{h_i}{2}$ ..... (35)

Hence,

$$B_{P11} = \frac{1}{c^2}\left[c_1\left(\frac{\partial N_i}{\partial x}\right) + c_2\left(\frac{\partial N_i}{\partial y}\right) + c_3\left(\frac{\partial N_i}{\partial z}\right)\right] \quad \text{..... (36)}$$

$$B_{P12} = \frac{1}{c^2}\left[c_2\left(\frac{\partial N_i}{\partial x}\right) + c_4\left(\frac{\partial N_i}{\partial y}\right) + c_5\left(\frac{\partial N_i}{\partial z}\right)\right] \quad \text{..... (37)}$$

$$B_{P13} = \frac{1}{c^2}\left[c_3\left(\frac{\partial N_i}{\partial x}\right) + c_5\left(\frac{\partial N_i}{\partial y}\right) + c_6\left(\frac{\partial N_i}{\partial z}\right)\right] \quad \text{..... (38)}$$

$$B_{P14} = \frac{\tilde{a}}{c^2}\left[\begin{array}{l}\left(\frac{\partial N_i}{\partial x}\right)\left(c_1 v_{1i}^x + c_2 v_{1i}^y + c_3 v_{1i}^z\right) + \left(\frac{\partial N_i}{\partial y}\right)\left(c_2 v_{1i}^x + c_4 v_{1i}^y + c_5 v_{1i}^z\right) + \\ \left(\frac{\partial N_i}{\partial z}\right)\left(c_3 v_{1i}^x + c_5 v_{1i}^y + c_6 v_{1i}^z\right)\end{array}\right] \quad \text{..... (39)}$$

$$B_{P15} = -\frac{\tilde{a}}{c^2}\left[\begin{array}{l}\left(\frac{\partial N_i}{\partial x}\right)\left(c_1 v_{2i}^x + c_2 v_{2i}^y + c_3 v_{2i}^z\right) + \left(\frac{\partial N_i}{\partial y}\right)\left(c_2 v_{2i}^x + c_4 v_{2i}^y + c_5 v_{2i}^z\right) + \\ \left(\frac{\partial N_i}{\partial z}\right)\left(c_3 v_{2i}^x + c_5 v_{2i}^y + c_6 v_{2i}^z\right)\end{array}\right] \quad \text{..... (40)}$$

The terms (B_{P11}, B_{P12}... B_{P15}) represent the first row of the embedded bar strain-displacement matrix [B_P].

Now, it is important to evaluate the values of (c_1, c_2, ...,c_6) and $c = |J_P|$. Noting that:

$$\frac{\partial x}{\partial \tau} = \frac{\partial x}{\partial \xi}\frac{\partial \xi}{\partial \tau} + \frac{\partial x}{\partial \eta}\frac{\partial \eta}{\partial \tau} + \frac{\partial x}{\partial \zeta}\frac{\partial \zeta}{\partial \tau} = J_{11}\frac{\partial \xi}{\partial \tau} + J_{21}\frac{\partial \eta}{\partial \tau} + J_{31}\frac{\partial \zeta}{\partial \tau} \quad \text{..... (41)}$$

$$\frac{\partial y}{\partial \tau} = \frac{\partial y}{\partial \xi}\frac{\partial \xi}{\partial \tau} + \frac{\partial y}{\partial \eta}\frac{\partial \eta}{\partial \tau} + \frac{\partial y}{\partial \zeta}\frac{\partial \zeta}{\partial \tau} = J_{12}\frac{\partial \xi}{\partial \tau} + J_{22}\frac{\partial \eta}{\partial \tau} + J_{32}\frac{\partial \zeta}{\partial \tau} \quad \text{..... (42)}$$

$$\frac{\partial z}{\partial \tau}=\frac{\partial z}{\partial \xi}\frac{\partial \xi}{\partial \tau}+\frac{\partial z}{\partial \eta}\frac{\partial \eta}{\partial \tau}+\frac{\partial z}{\partial \zeta}\frac{\partial \zeta}{\partial \tau}=J_{13}\frac{\partial \xi}{\partial \tau}+J_{23}\frac{\partial \eta}{\partial \tau}+J_{33}\frac{\partial \zeta}{\partial \tau} \quad \text{..... (43)}$$

$$\begin{Bmatrix}\frac{\partial x}{\partial \tau}\\ \frac{\partial y}{\partial \tau}\\ \frac{\partial z}{\partial \tau}\end{Bmatrix}=\begin{bmatrix}J_{11} & J_{21} & J_{31}\\ J_{12} & J_{22} & J_{32}\\ J_{13} & J_{23} & J_{33}\end{bmatrix}\begin{Bmatrix}\frac{\partial \xi}{\partial \tau}\\ \frac{\partial \eta}{\partial \tau}\\ \frac{\partial \zeta}{\partial \tau}\end{Bmatrix} \quad \text{..... (44)}$$

$$\begin{Bmatrix}\frac{\partial x}{\partial \tau}\\ \frac{\partial y}{\partial \tau}\\ \frac{\partial z}{\partial \tau}\end{Bmatrix}=[J]^{T}\begin{Bmatrix}\frac{\partial \xi}{\partial \tau}\\ \frac{\partial \eta}{\partial \tau}\\ \frac{\partial \zeta}{\partial \tau}\end{Bmatrix} \quad \text{..... (45)}$$

The shape functions of the embedded bar element are:

$$M_1=\frac{1}{2}\tau\,(\tau-1) \quad \text{..... (46)}$$

$$M_2=(1-\tau)^2 \quad \text{..... (47)}$$

$$M_3=\frac{1}{2}\tau\,(\tau+1) \quad \text{..... (48)}$$

Relating with **Fig.(2)**,

$$\xi=M_1\xi_1+M_2\xi_2+M_3\xi_3 \quad \text{..... (49)}$$

$$\xi=\frac{\tau^2}{2}(\xi_1-2\xi_2+\xi_3)+\frac{\tau}{2}(\xi_3-\xi_1)+\xi_2 \quad \text{..... (50)}$$

$$\eta=M_1\eta_1+M_2\eta_2+M_3\eta_3 \quad \text{..... (51)}$$

$$\eta=\frac{\tau^2}{2}(\eta_1-2\eta_2+\eta_3)+\frac{\tau}{2}(\eta_3-\eta_1)+\eta_2 \quad \text{..... (52)}$$

$$\zeta=M_1\zeta_1+M_2\zeta_2+M_3\zeta_3 \quad \text{..... (53)}$$

$$\zeta=\frac{\tau^2}{2}(\zeta_1-2\zeta_2+\zeta_3)+\frac{\tau}{2}(\zeta_3-\zeta_1)+\zeta_2 \quad \text{..... (54)}$$

The embedded bar stiffness can be determined as:

$$[K_P] = \int_v [B_P]^T E_P [B_P] \, dv \quad \text{..... (55)}$$

$$dv = A_P dL = A_P |J_P| d_\tau \quad \text{..... (56)}$$

where:

$[K_P]$: *is the stiffness matrix of embedded bar element,*

E_P: *is the modulus of elasticity of the embedded bar,*

A_P: *is the cross-sectional area of the embedded bar.*

4. Applications and Result

A nonlinear finite element computer program based on the degenerated shell element has been developed to include the above formulation in the representation of reinforcing steel bars in reinforced concrete members or prestressing tendons in prestressed concrete members. The program developed and used in this research work is based on the computer program PLAST by Huang [7].

In order to show the validity of the current formulation, the reinforced concrete plate tested experimentally by Duddeck et. al. [8] and numerically by Hinton and Owen [9] who used layered approach for steel modeling is considered using the embedded bar representation. A square reinforced concrete slab simply supported at four corners and loaded by a concentrated force at the center was tested by Duddeck et. al. [8], two slabs with different amounts of reinforcement in each direction (S1 and S2) are examined here. The slabs' geometry, amount of reinforcement and finite element discretization are shown in **Fig.(3)**, whereas, the material properties are presented in **Table (1)**.

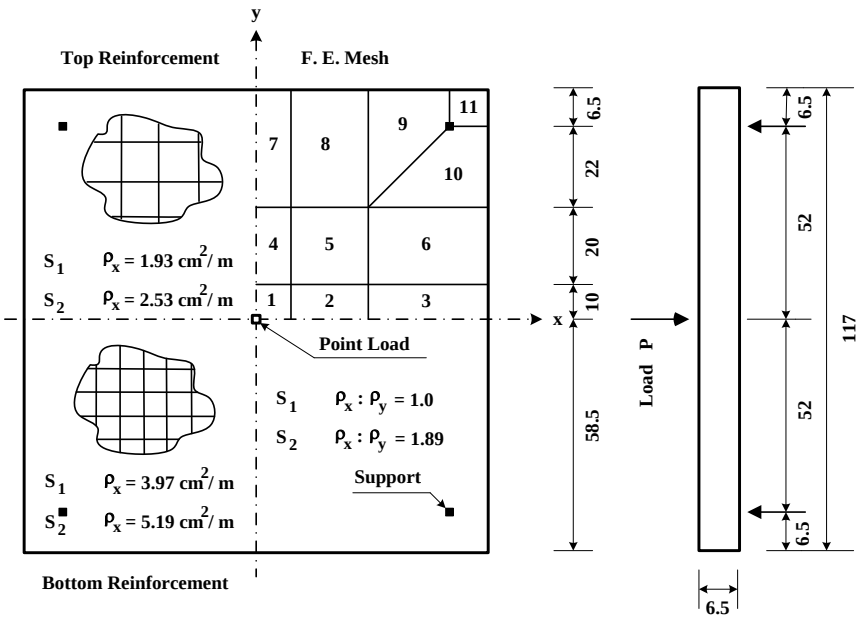

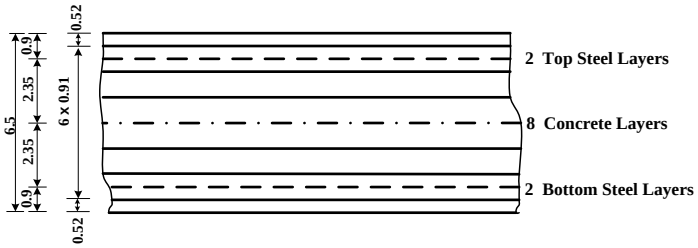

All dimensions in centimeters

Figure (3) Details and finite element idealization of Duddeck's square slab [8]

Table (1) Materials properties used by Duddeck et. al. [8]

Concrete		Reinforcing steel	
Young's modulus, E_c (MPa)	16400	Young's modulus, E_s(MPa)	201000
Compressive strength, f'_c (MPa)	43.0		
Tensile strength, f'_t (MPa)	3.0	Yield stress, f_{sy} (MPa)	600
Poisson's ratio, ν	0.0		
Ultimate compressive strain, ε_{cu}	0.0035	Hardening parameter, H' (MPa)	7250

By taking advantage of symmetry of loading and geometry, one quarter of the slab is modeled by a mesh of eleven degenerated shell elements, as shown in **Fig.(3)**. These elements are divided into eight-equal thickness concrete layers. Steel in the numerical analysis of Ref. [9] was modeled by four steel layers, as shown in **Fig.(3)**, whereas, in this investigation, the steel is modeled as embedded bars in the concrete elements. The numerical results for this slab have been obtained by applying the concentrated load on a small central area of 100x100 mm^2.

The computed load-deflection curve of the central point of slab S_1 is shown in **Fig.(4)**, along with the computed results of Ref. [9]. From this figure, it is seen that good agreement is obtained between the two results throughout the loading levels.

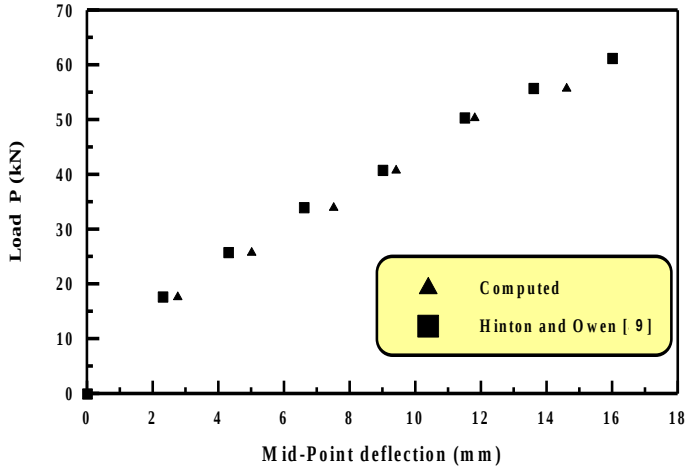

Figure (4) Comparison of computed load-central deflection curves for slab S_1

Comparison between the present computed deflections for slab S_2 and the experimental results by Duddeck et al.[8] and the numerical results of Ref. [9] is shown in **Fig.(5)**, which shows good agreement. The present computed ultimate loads of 58.5 kN and 41 kN for slabs S_1 and S_2, respectively, compared to the experimental ultimate load values of 61.25 kN and 43.5 kN also shows good agreement, in which the ratios of the predicted ultimate load to the experimental ultimate load are 0.955 and 0.953, respectively.

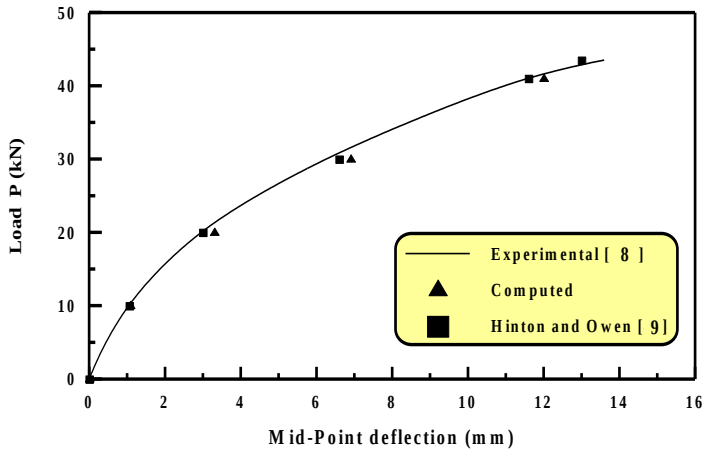

Figure (5) Comparison between computed and experimental central load-deflection curves for slab S_2

The proposed computer program is also used to analyze a two-way simply supported prestressed concrete slab, previously analyzed by Roca and Mari [10] and Van Greunen [11], this slab was originally tested experimentally by Ritz et. al. [12] The slab has a uniform thickness of 200 mm, the prestressing tendons have a parabolic profile reaching a maximum eccentricity of 65 mm at mid-span, and zero eccentricity at the ends. The geometry of the square simply supported slab and the layout of the prestressing tendons is shown in **Fig.(6)**, while material properties used in the analysis are given in **Table (2)**.

Also taking advantage of symmetry, one quarter of the slab is modeled using nine degenerated shell elements the slab is subjected to a uniformly distributed vertical load.

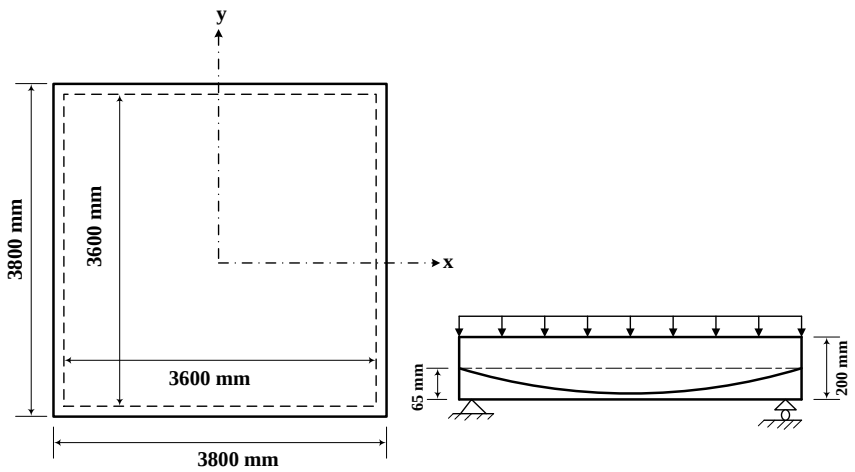

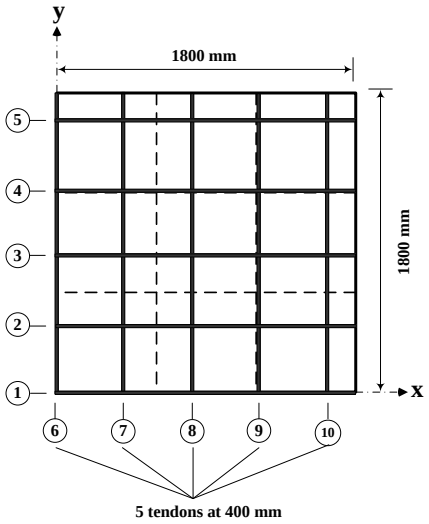

Figure (6) Details, geometry and layout of prestressing tendons of Ritz's et. al. [12] slab

Table (2) Materials properties used by Ritz et. al. [12]

Concrete		Prestressing tendons	
Young's modulus, E_c (MPa)	31920	Yield stress, f_{Py} (MPa)	979
Compressive strength, f'_c (MPa)	35	Ultimate stress, f_{Pu} (MPa)	1160
Tensile strength, f'_t (MPa)	3.5	Area of a prestressing tendon, A_P (mm^2)	92.9
Poisson's ratio, ν	0.18	Effective prestressing stress, σ_{Po} (MPa)	780
Ultimate compressive strain, ε_{cu}	0.002	Curvature friction coefficient μ (rad^{-1})	0.1
Unit weight, γ_c (kN/m^3)	25	Wobble friction coefficient κ (m^{-1})	0.00157

Figure (7), shows the computed and the experimental load-deflection curve for the center of the slab, from which, it is seen that good agreement between the two curves are obtained through most loading levels.

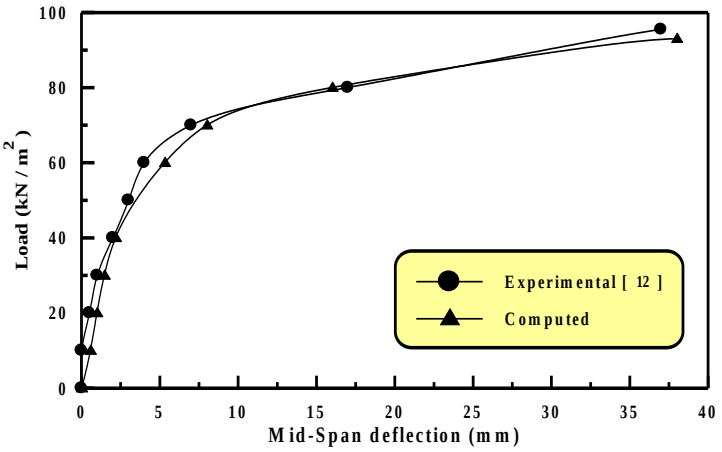

Figure (7) Comparison of computed and experimental load-deflection curves

Previous numerical results obtained by Roca and Mari [10] and Van Greunen [11] are drawn in **Fig.(8)** for comparison. The figure indicates that the present solution is the best in comparison with the experimental results.

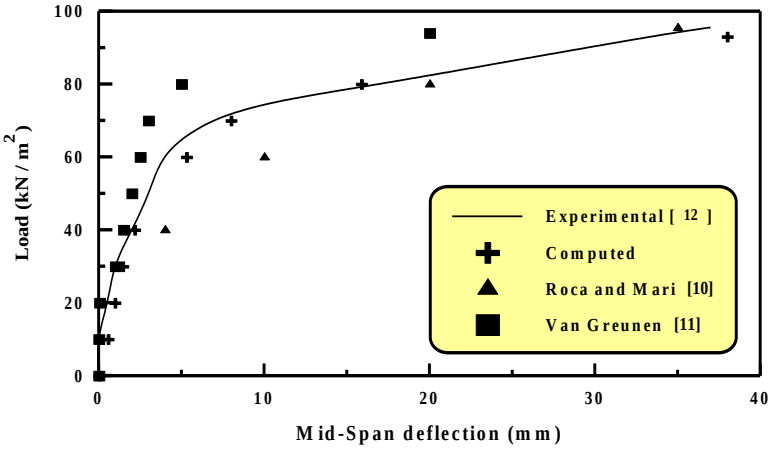

Figure (8) Comparison of computed load-central deflection curve with other numerical results

5. Conclusions

A new numerical formulation for representing of steel reinforcement bars and prestressing tendons as embedded bars in the degenerated shell element using finite element method is shown here in the present study. From the results of the finite element analysis carried out for both reinforced concrete and prestressed concrete slabs good agreement is found and proved that the used development for modeling prestressing tendons as embedded bars within the parent concrete element gave good results in comparison with the experimental results. Therefore, applying the prestressing force to each tendon is more realistic than considering the bar to be smeared.

However, the input file in the current case needs a little more effort in comparison with the other types of steel representations, i.e. smeared layer and discrete modeling, it is noticed from the analysis that, the bars positions within the concrete members must be located accurately, since their modeling as embedded bars in the present investigation need the correct location of each tendon with respect to the concrete parent element in the three coordinates of x, y, and z.

6. References

1. Ngo, D., and Scordelis, A., ***"Finite Element Analysis of Reinforced Concrete Beams"***, ACI Journal, Vol. 64, No. 3, 1967, pp. 152-163.

2. Arafa, M., and Mehlhorn, G., ***"A modified Discrete Model in the Nonlinear Finite Element Analysis of Prestressed and Reinforced Concrete Structures"***, 2nd International Ph.D. Symposium in Civil Engineering, Budapest, 1998.

3. Phillips, D. V., and Zienkiewicz, O. C., ***"Finite Element Nonlinear Analysis of Concrete Structures"***, Proceedings Institute of Civil Engineers, Part 2, Vol. 61, 1976, pp. 59-88.

4. Elwi, A. E., and Murray, D. W., ***"Nonlinear Analysis of Axisymmetric Reinforced Concrete Structures"***, Structural Engineering Report No. 87, University of Alberta, Edmonton, Alberta, Canada, 1980, Cited by Ref. [6].

5. Elwi, A. E., and Hurdey, T. M., ***"Finite Element Model for Curved Embedded Reinforcement"***, Journal of Engineering Mechanics, Vol. 115, No. 4, April, 1989, pp.740-753.

6. Ranjbaran, A., ***"Embeding of Reinforcements in Reinforced Concrete Elements Implemented in DENA"***, Computers and Structures, Vol. 40, No. 4, 1991, pp. 925-930.

7. Huang, H. C., ***"Static and Dynamic Analyses of Plates and Shells"***, Springer-Verlag U.K., 1st Ed., 1989.

8. Duddeck, H., Griebenow G., and Shaper, G., ***"Material and Time-Dependent Nonlinear Behavior of Cracked Reinforced Concrete Slabs"***, in ***"Nonlinear Behavior of Reinforced Concrete Spatial Structures"***, Vol. 1, Preliminary Report IASS Symposium held in Darmstadt, Eds. G. Mehlhorn, H. Ruhle and W. Zerna, Werner-Verlag Dusseldorf, pp. 101-113, July 1978, Cited by Ref. [9].

9. Hinton, E., and Owen, D. R. J, ***"Finite Element Software for Plates and Shells"***, Pineridge Press U.K., 1st Ed., 1984.

10. Roca, P., and Mari, A. R., ***"Nonlinear Geometric and Material Analysis of Prestressed Concrete General Shell Structures"***, Journal of Computers and Structures, Vol. 46, No. 5, May 1993, pp. 917-929.

11. Van Greunen, J., ***"Nonlinear Geometric, Material and Time Dependent Analysis of Reinforced and Prestressed Concrete Slabs and Panels"***, University of California, Berkeley, UC-SESM Report No. 77-3, 1979.

12. Ritz, P., Mari, P., and Thürlimann, B., ***"Versuche über das Biegeverhalten von Vorgespannten Platten ohne Verbund"***, Institute für Baustatik and Konstruktion, Zurich, Report No. 7305-1, 1975, Cited by Ref. [10].

Notations

A_P =	Cross-Sectional area of prestressing tendon
$[B_P]$=	Strain-Displacement matrix of prestressing tendon
E_c =	Modulus of elasticity of concrete
E_P =	Modulus of elasticity of prestressing tendon
E_s =	Modulus of elasticity of reinforcement steel
h_k =	Shell thickness at node k
$[\mathbf{J_P}]$ =	Jacobian matrix of prestressing tendon
$[K_P]$ =	Prestressing tendon stiffness matrix
M_1, M_2, M_3 =	Shape functions of the embedded bar
N_k =	Shape function at node k
u, v, w =	Displacement in global x, y, z-direction
$\mathbf{v_{1k}, v_{2k}, v_{3k}}$ =	Nodal Cartesian coordinate system at node k
x, y, z =	Global Cartesian coordinate system
$\mathbf{x', y', z'}$ =	Local Cartesian coordinate system
$\boldsymbol{\varepsilon}$ =	General strain
τ =	Dimensionless coordinate along the embedded bar element
ξ, η, ζ =	Natural coordinate system